Initial measurements of plasma current and electron density profiles using a polarimeter/interferometer (POINT) for long pulse operation in EAST (invited)

H. Q. Liu, J. P. Qian, Y. X. Jie, W. X. Ding, D. L. Brower, Z. Y. Zou, W. M. Li, H. Lian, S. X. Wang, Y. Yang, L. Zeng, T. Lan, Y. Yao, L. Q. Hu, X. D. Zhang, and B. N. Wan

---

Articles you may be interested in

Faraday-effect polarimeter-interferometer system for current density measurement on EAST
Review of Scientific Instruments **85**, 11D40511D405 (2014); 10.1063/1.4889777

Measurement of local, internal magnetic fluctuations via cross-polarization scattering in the DIII-D tokamak (invited)
Review of Scientific Instruments **87**, 11E60111E601 (2016); 10.1063/1.4960154

Optical configuration optimization and calibration for the POINT system on EAST
Review of Scientific Instruments **87**, 11E12111E121 (2016); 10.1063/1.4961272

Initial measurements of plasma current and electron density profiles using a polarimeter/interferometer (POINT) for long pulse operation in EAST (invited)

H. Q. Liu,[1] J. P. Qian,[1,a)] Y. X. Jie,[1] W. X. Ding,[2] D. L. Brower,[2] Z. Y. Zou,[1] W. M. Li,[1] H. Lian,[1] S. X. Wang,[1] Y. Yang,[1] L. Zeng,[1] T. Lan,[1,3] Y. Yao,[1] L. Q. Hu,[1] X. D. Zhang,[1] and B. N. Wan[1]

[1]*Institute of Plasma Physics, Chinese Academy of Sciences, Hefei, Anhui 230031, People's Republic of China*
[2]*Department of Physics and Astronomy, University of California Los Angeles, Los Angeles, California 90095, USA*
[3]*University of Science and Technology of China, Hefei, Anhui 230026, People's Republic of China*

A double-pass, radially viewing, far-infrared laser-based POlarimeter-INTerferometer (*POINT*) system utilizing the three-wave technique has been implemented for diagnosing the plasma current and electron density profiles in the Experimental Advanced Superconducting Tokamak (EAST). POINT has been operated routinely during the most recent experimental campaign and provides continuous 11 chord line-integrated Faraday effect and density measurement throughout the entire plasma discharge for all heating schemes and all plasma conditions (including ITER relevant scenario development). Reliability of both the polarimetric and interferometric measurements is demonstrated in 25 s plasmas with H-mode and 102 s long-pulse discharges. Current density, safety factor (q), and electron density profiles are reconstructed using equilibrium fitting code (EFIT) with POINT constraints for the plasma core. *Published by AIP Publishing.* [http://dx.doi.org/10.1063/1.4963378]

I. INTRODUCTION

Achievement of long pulse and steady-state plasma regimes is a major challenge for both ITER and prospective fusion power reactors. A primary goal of the Experimental Advanced Superconducting Tokamak (EAST) device is to develop long-pulse high-performance plasmas near the operational [magneto-hydro-dynamic (MHD) and beta] limits using ITER relevant actuators [neutron beam injection (NBI), RF current drive, and heating] and sensors. The goal of plasma discharge extension to long pulse is important for demonstrating that the current profile relaxes to a steady-state, and that no stability boundary is crossed during this evolution that would compromise performance. This requires an accurate, time-resolved diagnosis of the internal magnetic field, current density, and electron density profiles. Measuring the Faraday effect is an appealing candidate for internal magnetic field measurement as no neutral beams are required, and information is provided continuously throughout the entire plasma discharge. In addition, high temporal resolution measurements provided are indispensable for advanced tokamak operation as tracking fast equilibrium profile dynamics and magnetic field fluctuations can be utilized for plasma control. Polarimeter systems, with either poloidal, vertical, or toroidal viewing geometry, have been successfully demonstrated on many devices, including TEXTOR,[1] TEXT,[2]

JET,[3] MST,[4] and Alcator C-Mod.[5] A laser-based, double-pass, radially viewing, 11 channel Faraday effect POlarimetry-INTerferometry (*POINT*) diagnostic has been developed for current density and electron density profile measurements in the EAST tokamak.[6,7] POINT, which provides a non-perturbing probe of the core magnetic and current density profiles of high-performance plasmas, will focus on real-time plasma control for up to 1000 s discharges in order to extend high-performance plasma regimes to long-pulse and develop ITER-like scenarios. The realtime output of POINT will be used to monitor the fast profile dynamics of electron density, current density, and q (safety factor) and ultimately be integrated into the real-time plasma control system. Since the 2015 experimental campaign, the 11 channel POINT system has been routinely operated to measure the electron density, current density, and safety factor profiles for long-pulse EAST plasmas. In this paper, we present the instrumental technique, optical layout, calibration, and initial experimental results from the 11-chord POINT system. Initial equilibrium electron density, current density, and q profiles are obtained from equilibrium reconstruction using equilibrium fitting code (EFIT) with POINT constraints. Measurements clearly demonstrate the low phase noise and fast time response (up to 4 μs) of POINT thereby enabling the observation of both equilibrium dynamics and small-amplitude fluctuations.

II. POINT ON EAST

A. POINT with three-wave technique

The three-wave configuration has been demonstrated to work successfully on several plasma experiments including

---

RTP,[8] MST,[4] J-TEXT,[9] and Alcator C-Mod.[5] EAST POINT[6,7] is configured using double-pass, radially viewing chords which access the plasma via an equatorial mid-plane port. An initial five-chord test system installed in 2014 was upgraded to 11 chords in 2015. The horizontal chords are situated at vertical locations above and below the mid-plane with z = −42.5, −34, −25.5, −17, −8.5, 0, 8.5, 17, 25.5, 34, 42.5 cm (0 cm denotes the vacuum vessel center). An overview of the optical layout is provided in Fig. 1. Three CW far-infrared gas lasers using formic acid (HCOOH) and operating at nominal wavelength 432.5 μm are used as the sources. Each far infrared (FIR) laser is optically pumped by independent infrared CO_2 lasers operating at 9.27 μm on the 9R20 line with power ~50 W. FIR output power is up to 30 mW per cavity. Two lasers, with slight frequency offset (~1 MHz), are made collinear with counter-rotating circular polarization (R- and L-waves) in order to determine the Faraday effect by measuring their phase difference upon transmission through the plasma,

$$\Psi_F = \frac{2\pi}{\lambda} \int \frac{(n_R - n_L)}{2} dz$$
$$= 2.62 \times 10^{-13} \lambda^2 \int n_e(z) B_\parallel(z) dz, \qquad (1)$$

where λ is the laser wavelength, dz is the plasma path length, and $B_\parallel$ in Tesla is the magnetic field component along the beam. The Faraday effect is half the phase difference between the two beams. The third laser, also slightly frequency offset, is used as a reference providing local oscillator (LO) power to each detector so that one can obtain the phase shift caused by the plasma R- and L-waves separately. The electron density is obtained by taking the average of these two quantities according to the relation

$$\Phi = \frac{2\pi}{\lambda} \int \frac{n_R + n_L}{2} dz \approx 2.82 \times 10^{-15} \lambda \int n_e(z) dz. \quad (2)$$

All waves are detected using Virginia Diodes, Inc. (VDI) Schottky planar-diode fundamental waveguide mixers with integrated conical horn optimized for high sensitivity, 750 V/W. This is sufficient to provide good signal quality for all 11 chords and reference of the polarimeter-interferometer system.

The triple laser system is positioned on an optical table (weighing ~20 tons) located in a humidity and temperature-controlled room outside the machine hall. The laser room provides a thermostatic, vibration-free, electromagnetic shielded environment for lasers. On the optical table, two FIR laser beams are combined making them spatially overlapped and collinear with orthogonal linear polarization. The combined beams are guided to the optical tower in the EAST machine hall, together with the linearly polarized LO beam using separate overmoded, dielectric waveguides of ~20 m length. Optical stability is an important issue for FIR optical diagnostics. To minimize vibration caused by the tokamak environment, a massive stainless steel tower (weighing ~30 tons), mechanically independent of the EAST machine, is constructed to ensure the stability of beam-processing optics. All optical components (mirrors, beam splitters, waveplates, lens, etc.), including the mixers and heterodyne receiver system, are mounted on an optical breadboard attached to this tower. The optical tower is located immediately adjacent to the EAST tokamak, by the diagnostic access port for the POINT system. It has been observed that mechanical vibration errors decrease up to two orders with the highly stable optical table and tower. The probe beams are divided into 11 individual chords and a reference using wire-mesh beam splitters. Probe beams for each chord are converted to orthogonal, counter-rotating circular polarization by a quarter waveplate before entering the plasma.

The two probe beams are combined with the LO beam after a double pass through the plasma achieved by reflecting from corner-cube retro-reflectors (RR) mounted on the inside wall of EAST. The beams are then focused onto the mixers where signals are observed at the difference or intermediate frequencies (IFs) of the lasers in the 1-2 MHz range. All intermediate frequency signals are processed by an amplifier and filter module and then sent into a high-speed digital phase detector (DPD) to extract the phase shift information, from which Faraday rotation angle and density phase shift can be obtained. The raw waveforms measured by each mixer are also digitized at 10 MHz and stored for postdischarge processing using a software-based demodulation algorithm.

B. Key components

For the POINT system, in-vessel molybdenum retro-reflectors (RR) with 50 mm aperture are the major component determining the Gaussian beam size along the laser path. The surfaces of these RR are aligned with accuracy up to 20 arcs to ensure high quality of the return beams. In addition, the retro-reflectors are designed to withstand baking temperatures up to 350 °C and discharge duration of more than 1000 s without surface distortion. After two months of experimental operation on EAST, the mirror surface of the RR was coated by a 36 μm film due to long time exposure to plasma discharges, as shown in Fig. 2. Tests of the film coating materials reveal the sample includes 14% carbon, 79.5% oxygen, 0.5% silicon, 0.8% ferrum, and 5.2% molybdenum. The FIR probe beam signal reflected from the RR was recorded over a period of ~60 days, from March 10th to May 5th, where a gradual decrease was observed in the detected signal amplitude, but sufficient power remained to conduct the POINT measurements of electron density and Faraday rotation. During this operation, it was
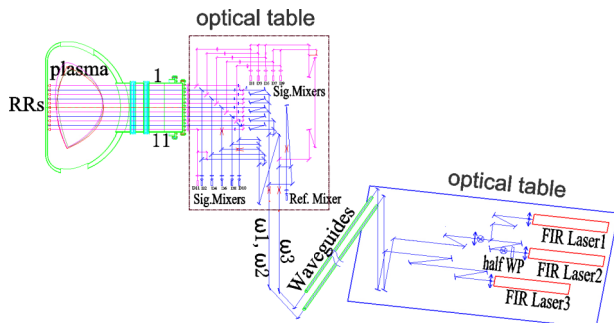

FIG. 1. 11 channel optical layout of the EAST POINT system, 5 channels (blue) are installed in 2014 with expansion to 11 channels (with added 6 channels in pink) in 2015.
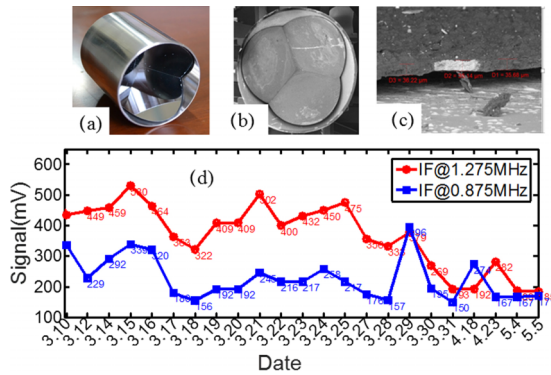
FIG. 2. (a) New retro reflector, (b) retro reflector with film coating after two months used, (c) film on retro reflector, and (d) reflected signal by retro-reflector versus date.

also noted that no distortion of the FIR beam polarization was observed as determined from the system calibration. Despite the surface degradation of the RR, POINT was able to continue making measurements. It is speculated that much of the RR surface damage may occur during the discharge cleaning process, and future plans call for adding shutters to protect the RR from this exposure.

The long term goal of the EAST program is to use POINT data, in conjunction with other diagnostic systems, for realtime feedback control in order to maintain stable operation of high-performance tokamak plasmas while avoiding deleterious MHD events such as disruptions and edge localized modes (ELMs). Stable intermediate frequencies (IFs) among the three FIR lasers are required for reliable real-time output of the electron density and current density to meet this requirement. To that end, a closed-loop control system is developed to stabilize the FIR laser IFs at a pre-set value based on an automatic control of the FIR laser cavity length using a piezo-electric transducer (PZT). A stable IF signal over a long time period (up to several hours) is obtained using this frequency control system. The output IF drift is lower than 0.6% for a 1 h (3600 s) test. In addition, each CO_2 pump laser is frequency locked to a Fabry-Perot cavity.

Meanwhile, a Digital Phase Detector (DPD), prototype hardware based on a Peripheral Component Interconnect (PCI) card that utilizes a very high speed Field Programmable Gate Array (FPGA), has been developed to provide realtime output with 250 kHz bandwidth for POINT system. The DPD is used to perform phase demodulation and real-time phase calculations, provides real-time Faraday rotation angle and density phase shift output for use in the EAST plasma control system. Real-time EFIT with Faraday angle and density phase shift constraints is planned for implementation in the plasma control system in the near future. The DPD samples the reference and plasma signals each containing the three IF bands of information, currently centered at 0.850, 1.275, and 2.125 MHz with about a 100 kHz variation tolerance. With input signals from the plasma and reference mixers, DPD output for each chord corresponds to the plasma density (0.85 MHz) and Faraday-effect (1.275 MHz). Since the phase difference between the R- and L-waves (Faraday effect) is small, we can directly use the R- or L-waves to determine the plasma density while only introducing a 1% error. Laser

stability is necessary for POINT operation with the long term goal to provide real-time input to the plasma control system.

C. POINT system errors

Measurement accuracy is directly determined by the identification and minimization of RMS and systematic errors. For interferometric measurement, mechanical vibration is a major error source which can easily induce error up to tens of degrees. As mentioned before, EAST POINT employs a massive, stable optical table and optical tower to decrease the mechanical error by up to two orders. After first alignment, *in situ* test without plasma reveals the electron density error is lower than 5×10^{16} m^{-2} (2°), while the Faraday rotation angle RMS phase noise is <0.1°. For polarimetric measurement, systematic errors come from non-collinear (spatially offset) probe beams, polarization distortion from non-ideal optical components, instability of intermediate frequency, misalignment to the toroidal field, finite-temperature effects, Cotton-Mouton effect, and geometric phase effects. The finite-temperature effects, IF stability (with feedback control), Cotton-Mouton effect, and geometric phase effects are less than the RMS noise level of POINT. During EAST operation, the toroidal field direction was reversed, and amplitude scanned from 1.6 T to 2.8 T, and no misalignment to toroidal field was detected. The remaining polarization and collinearity errors are the major source of systematic errors for EAST POINT and will be discussed in more detail.

The polarization distortion results from non-ideal optical components primarily resulting from wire-mesh beam splitter reflectance and transmission that is polarization sensitive. Distortion of laser beam circular polarization due to anisotropic reflectivity/transmissivity of optics is largely eliminated by a newly developed optical configuration optimization. Calibration techniques for the double-pass system with zero-offset return beam have been developed, confirming polarization conservation.[10] For examining the polarization of counter-rotating circularly polarized probe beams, we add a rotating half-wave plate in the optical path to replace the plasma and modulate the polarization. If the probe beams' polarizations are counter-rotating circularly polarized, phase difference between the R- and L-waves will change linearly and equal four times the rotation angle of the half-wave plate; any distortion of polarization will lead to a nonlinear response. As shown in Fig. 3(a), a linear calibration curve is observed indicating very small distortion of the probe beam polarization throughout the optical system. This calibration procedure is followed for each chord of the POINT system.

The second important source of systematic error stems from non-collinearity and/or non-matched spatial overlap of the probe beams and is a unique issue to three-wave measurement technique. When the L-wave and R-wave are not collinear, phase error will be introduced by the difference of their optical path length and the different plasma regions probed in the presence of a finite density gradient according to $\frac{\Delta\phi_R - \Delta\phi_L}{2} = \Psi_F + c_i \int \nabla n_e \cdot \Delta z \, dz$, where c_i is a constant. The collinearity error can be directly detected by placing a linear polarizer in the probe beam path prior to passing through the plasma. In this configuration, any phase difference
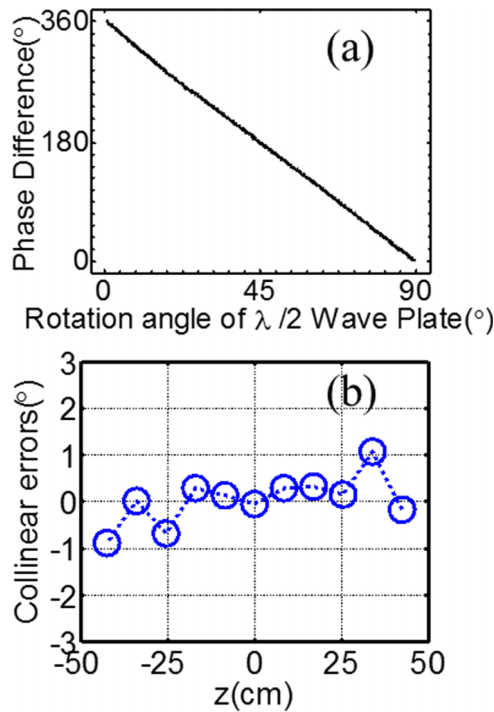
FIG. 3. Calibration results of (a) polarization of probe beams and (b) collinear error for 11 chords in high density EAST experiment.
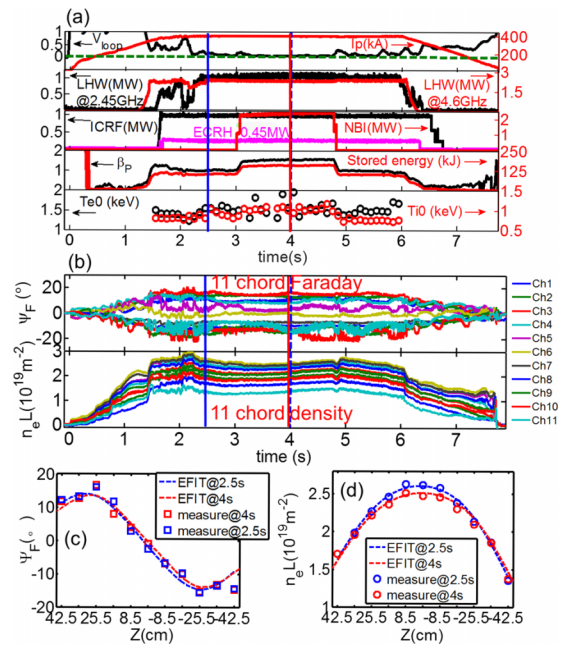

FIG. 4. Typical plasma discharge (shot No. 62295) results from EAST POINT. (a) Typical plasma parameter, (b) 11 chord Faraday angle and 11 chord line-integrated density, (c) Faraday angle, and (d) line-integrated density at t = 2.5 s and t = 4 s.

measured between the two probes that now have the same polarization must result from the beam misalignment or non-spatial overlap. The collinearity error can be directly examined in plasma experiment and is shown in Fig. 3(b), for a typical EAST discharge. All 11 chords are used in the test to obtain the error profile where the central line-averaged density for this case is 3×10^{19} m^{-3}. As shown in the figure, the collinearity error is less than $0.3°$ for almost all chords, smaller than the Faraday angle. Chords positioned nearer the plasma edge where the density gradient is steepest show the largest error as expected.

III. EXPERIMENTAL RESULTS

Prior to the most recent EAST experimental campaign, POINT system alignment and calibration were optimized. The phase resolution for each of the 11 chords is about $0.1°$ for Faraday rotation angle and about $1°$ for line-integrated density phase averaged within a bandwidth of 50 kHz. An example of 11-chord measured data from the EAST POINT is presented in Fig. 4. The discharge is a high-performance H-mode plasma with 2.4 MW neutron beam injection (NBI), $B_T = 2.5$ T, $I_p = 400$ kA, $T_{e0} = 2$ keV, $T_{i0} = 1.5$ keV, central line average density 3×10^{19} m^{-3}, $\beta p = 1.5$, stored energy = 155 kJ, and $V_{loop} = 0$, as shown in Fig. 4(a). The injection heating power includes 2.4 MW NBI, 1 MW ion cyclotron resonance heating (ICRH), 0.45 MW electron cyclotron resonance heating (ECRH), 2.3 MW low hybrid wave (LHW) at 4.6 GHz, and 1 MW LHW at 2.45 GHz. Fig. 4(b) shows the temporal evolution of the actual line-integrated density and Faraday effect measurements exhibiting no obvious interference from powerful NBI, LHW, ICRH, and ECRH heating sources,

indicating that POINT can operate for any heating scheme employed on EAST. In addition, it is important to note that the known phase error associated with movement of the RR is not detected in the density phase measurement. This indicates that the phase error is too small to be identified because the movement of the RR is very small compared to the 432.5 μm wavelength of the probe beams. Figs. 4(c) and 4(d) show the profiles of measured 11 chord Faraday angle and line-integrated density, respectively. The Faraday effect profiles change sign above and below the plasma midplane due to the change in the poloidal field direction. The line-integrated density profile is centrally peaked. Due to the fast time response and excellent phase resolution of POINT, no fringe counting errors or fringe skips are observed in the density phase data. Typically less than 1% of EAST discharges exhibit any fringe counting errors by using the DPD, with providing the lasers are tuned, and the mixer signal levels are sufficient to maintain a good signal-to-noise ratio. Some modulations of Faraday rotation angle phase exist during the density ramp up and ramp down, as shown in Fig. 4(b). The phase of this modulation is related to the phase shift due to plasma ϕ_{int}, measured with the interferometer. One of the causes of these modulations is the optical back talk, which is multi-reflection between detector and optical components, between polarimeter and interferometer due to the double pass optical configuration. The amplitude of the modulations of each channel is different because the optical back talk and ϕ_{int} are different in each channel. During the plasma platform, the plasma density is not so change, the modulation of Faraday rotation angles is very weak. So POINT system can provide good Faraday rotation angle during plasma platform.

A comprehensive method to self-consistently reconstruct the current and density profiles with magnetic and POINT
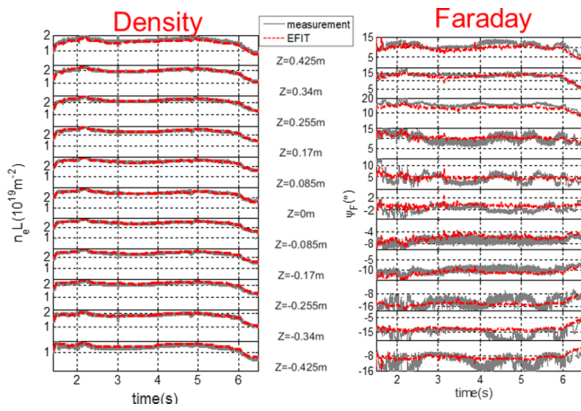
FIG. 5. Typical EFIT equilibrium with POINT constraints. Overplotted using dashed lines are results from POINT measurement and EFIT reconstruction. (left) Line-averaged density by POINT measurement (solid grey lines) and inverse integrated analysis by using EFIT reconstructed (dashed red lines), (right) line-integrated Faraday rotation angle by POINT measurement (solid grey lines) and inverse integrated analysis by using EFIT reconstructed (dashed red lines).

measurements by using the equilibrium fitting code EFIT was developed.[11,12] The measured line-integrated profiles are compared with the results computed from EFIT (magnetic equilibrium reconstruction) for 11 channels at times t = 2.5 s (L mode) and t = 4 s (H mode). Figure 5 shows the time evolution of the actual line-integrated density measurements and Faraday rotation measurements as compared with the results computed from EFIT (magnetic equilibrium reconstruction with POINT constraints) for 11 channels. At each chord location, the measurements are consistent with EFIT estimates of line average density and the Faraday angle within experimental error. This agreement also supports the claim that the toroidal magnetic field is having no deleterious effect on the measurements via either misalignment or the Cotton-Mouton effect.

The local current, density, and safety factor (q) profiles are obtained from equilibrium reconstruction using the EFIT code constrained by measurements from external magnetic coils and POINT. The electron density, current density, and safety factor (q) profiles for the discharge discussed in Fig. 5 and are shown in Fig. 6. Here we see that the density profile is broad and centrally peaked whereas the current density profile becomes hollow during NBI heating (3 s–5 s), leading to identification of reverse shear q profile in EAST. Also the stored energy increases from 90 kJ to 140 kJ, and the plasma confinement is improved with reverse shear q profile during NBI heating.

The POINT chords are positioned about the plasma core and provide the strongest constraint in the region where the plasma current is maximum. Further validation of POINT measurements related to the plasma q value and q = 1 surface position has been explored. Sawteeth is a Magneto-Hydro-Dynamic (MHD) instability in the core plasma region, which is often observed by electron cyclotron emission (ECE) and soft X-ray (SXR) diagnostics. The existence of sawteeth is generally associated with $q_{min} < 1$, while the radius of q = 1 rational surface can be approximated by the sawtooth inversion radius. EFIT magnetic equilibrium reconstruction using only constraints from the external magnetic coil data,
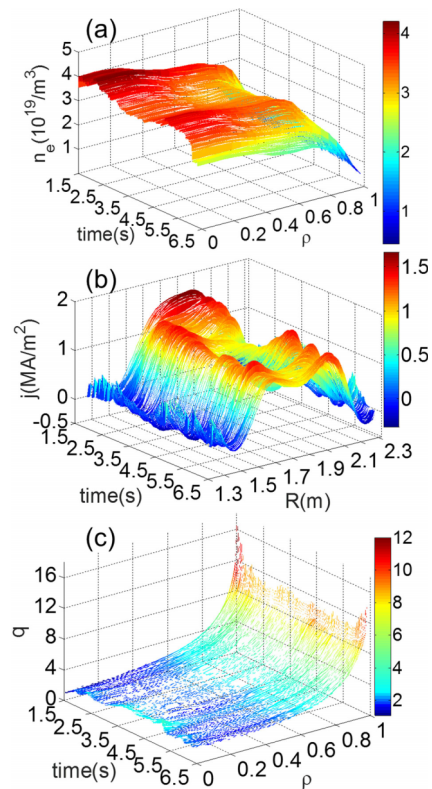

FIG. 6. Time evolution of (a) electron density profile, (b) plasma current profile, and (c) safety factor (q) profile reconstructed by EFIT constrained by POINT data.

indicates that q > 1, with or without sawtooth activity in the plasma, see Fig. 7. After adding the POINT constraints to EFIT, the safety factor decreases such that $q_{min} < 1$ during the sawtooth phase of the discharge, as shown in Fig. 7. When the sawtooth activity stops, the q_{min} value rises above 1. This result demonstrated the importance of the POINT constraints of the equilibrium reconstruction. Without internal measurement constraints provide by POINT, the EFIT result is not able to accurately determine the core q value.

For the plasma discharge data shown in Fig. 4, at t = 4 s the core electron temperature increases significantly up to 2 keV, higher than 1.5 keV before 3 s (Fig. 4(a)). The importance of adding POINT constraints to EFIT reconstruction is clearly seen in Fig. 8(a), at t = 4 s. Without internal
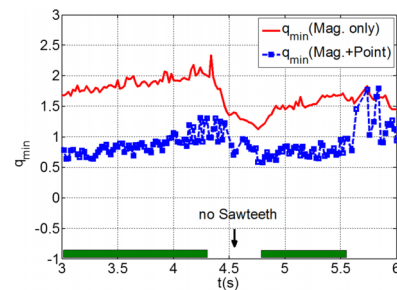

FIG. 7. q_{min} evolution during sawteeth activity. q_{min} by using EFIT reconstructed with only magnetic coils data (red solid line), EFIT reconstructed with magnetic coils data and POINT data (blue dashed line with rectangle). The green colorbar means sawteeth events identified by ECE and SXR diagnostics, shot No. 51063.
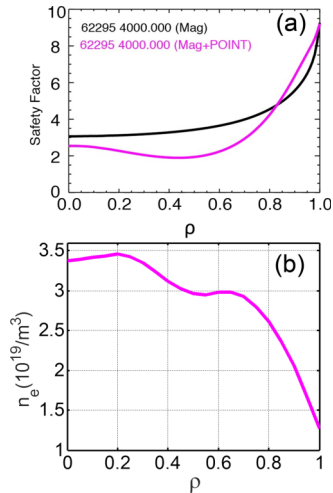
FIG. 8. Reverse shear q profile with ITB-like structure. (a) Reverse shear q profile by EFIT constrained by POINT data, (b) electron density profile by POINT with ITB-like structure.

FIG. 10. 102 s long-pulse discharges with Te0 > 4.5 keV, shot No. 59892.

constraints provide by POINT, EFIT is unable to resolve the hollow current profile leading to a reversed shear q-profile. When the reversed shear condition develops in EAST, the electron density and temperature profile peak suggesting the possible presence of an internal transport barrier (ITB)-like structure, as shown in Fig. 8(b). From these data it becomes clear that initial 11 chord POINT provides a important information for determination of the current and q profiles for the EAST tokamak. POINT can also be used in conjunction with MSE measurements and other internal information to provide better constraints for equilibrium reconstruction in future.

Fig. 9 shows the Faraday-effect and density fluctuation spectrographs obtained from POINT for chords situated at $Z = 25.5$ cm. It is indicated that not only the density fluctuations measured by interferometer but also the poloidal field fluctuations measured by polarimeter can be clearly observed by the high temporal resolution measurements provided by POINT. It is indispensable for investigating the role of magnetic fluctuations (tearing modes, NTMs, fast-particle driven instabilities) on plasma equilibrium and performance.

Another measurement example from POINT is shown in Fig. 10. Here we see a 102 s long plasma discharge with high electron temperature of more than 4.5 keV, $B_T = 2.8$ T, Ip= 400 kA, and central density 2×10^{19} m^{-3} for lower single null configuration using a graphite divertor. The injection heating power includes 0.4 MW ECRH, 1.3 MW LHW at 4.6 GHz and 0.5 MW LHW at 2.45 GHz, and 0.3 MW NBI. In Figure 10, the green line is the density signal from POINT central channel, and the blue line is the Faraday rotation angle from POINT channel 5. Similar data are obtained from all the POINT chords for this shot. These data demonstrate that POINT provides continuous current and density profile measurement information during the entire discharge period, over 100 s, with microsecond time response able to detect MHD events.

IV. SUMMARY AND FUTURE PLAN

An 11-chord, double-pass, radially viewing, polarimeter-interferometer system has been developed and now routinely operated from 2015 to diagnose the core region of EAST plasmas. A digital phase detector with 250 kHz bandwidth, which provides real-time Faraday rotation angle and density phase shift output for use in plasma control, has been developed for the POINT system. The electron line-integrated density resolution of POINT is better than 1×10^{16} m^{-2} ($<1°$), the Faraday rotation angle RMS phase noise is $<0.1°$, and high temporal resolution, up to ~ 1 μs, is achievable. Reliability of both the polarimetric and interferometric measurements is demonstrated during H mode discharges with four sources of auxiliary heating. Large density gradients present during H-mode operation do not negatively impact POINT measurements and POINT works for all heating schemes tested on EAST to date. The POINT system works well with 102 s long pulse discharge showing that it can provide continuous current and density profile measurements required for realtime plasma control. The initial current profile, density profile, and safety factor (q) profile are reconstructed using the EFIT code. Comparison of EFIT output constrained by POINT data shows good agreement with measurements serving to validate POINT data. POINT measurements can now be used to investigate plasma confinement and transport issues related to reversed magnetic shear and ITB-like
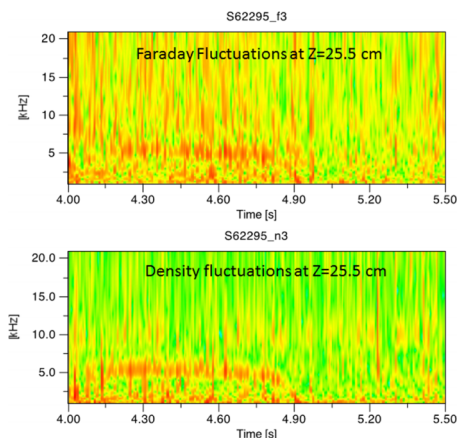

FIG. 9. (Top) Faraday fluctuations spectrograph and (bottom) density fluctuations spectrograph of the faraday angle and line-integrated density signal of POINT at $Z = 25.5$ cm.
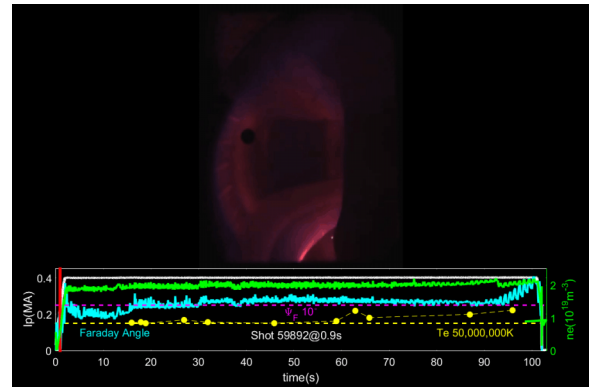
structures. Future plans include the integration of POINT measurements into real-time EFIT (rtEFIT). Long term goals include using POINT data, in conjunction with other diagnostic systems, for feedback control in order to maintain stable operation of long-pulse, high-performance tokamak plasmas while avoiding deleterious MHD events such as disruptions and ELMs. The edge polarimeter/interferometer will be developed for the bootstrap current measurement and edge current constraints. Edge current information could be more accurately reconstructed by kinetic EFIT together with pressure profile, which could be provided by Thomson scattering, reflectometry, and edge polarimeter/interferometer in future.

ACKNOWLEDGMENTS

[1]H. Soltwisch, Rev. Sci. Instrum. **57**, 1939 (1986).
[2]L. Zeng, D. L. Brower, and Y. Jiang, Plasma Phys. Controlled Fusion **39**, 591–608 (1997).
[3]G. Braithwaite *et al.*, Rev. Sci. Instrum. **60**, 2825 (1989).
[4]W. X. Ding *et al.*, Rev. Sci. Instrum. **81**, 10D508 (2010); D. L. Brower, W. X. Ding, S. D. Terry *et al.*, *ibid.* **74**, 1534 (2003).
[5]W. F. Bergerson *et al.*, Rev. Sci. Instrum. **83**, 10E316 (2012).
[6]H. Q. Liu *et al.*, Rev. Sci. Instrum. **85**, 11D405 (2014).
[7]H. Q. Liu *et al.*, J. Instrum. **11**, C01049 (2016).
[8]J. H. Rommers *et al.*, Rev. Sci. Instrum. **68**, 1217 (1997).
[9]J. Chen *et al.*, Rev. Sci. Instrum. **85**, 11D303 (2014).
[10]Z. Y. Zou *et al.*, Rev. Sci. Instrum. **87**, 11E121 (2016).
[11]J. Qian *et al.*, Plasma Sci. Technol. **17**, 75 (2015).
[12]J. Qian *et al.*, "EAST equilibrium current profile reconstruction using polarimeter-interferometer internal measurements," Nucl. Fusion (submitted).